International Journal of Pharmaceutics 416 (2011) 453–460

Contents lists available at ScienceDirect

International Journal of Pharmaceutics

journal homepage: www.elsevier.com/locate/ijpharm

Selegiline-functionalized, PEGylated poly(alkyl cyanoacrylate) nanoparticles: Investigation of interaction with amyloid-β peptide and surface reorganization

Benjamin Le Droumaguet[1], Hayfa Souguir[1], Davide Brambilla, Romain Verpillot, Julien Nicolas*, Myriam Taverna, Patrick Couvreur, Karine Andrieux**

Laboratoire de Physico-Chimie, Pharmacotechnie et Biopharmacie, Univ. Paris-Sud 11, UMR CNRS 8612, Faculté de Pharmacie, 5 rue Jean-Baptiste Clément, 92296 Châtenay-Malabry, France

ARTICLE INFO

Article history:
Received 29 October 2010
Received in revised form
28 December 2010
Accepted 5 January 2011
Available online 18 January 2011

Keywords:
Alzheimer's disease
Selegiline
Amyloid-β peptide
Poly(alkyl cyanoacrylate) nanoparticles
Functionalization

ABSTRACT

Alzheimer's disease (AD) is a neurodegenerative disorder for which the research of new treatments is highly challenging. Since the fibrillogenesis of amyloid-β peptide 1–42 ($A\beta_{1-42}$) peptide is considered as a major cause of neuronal degeneration, specific interest has been focused on aromatic molecules for targeting this peptide. In this paper, the synthesis of selegiline-functionalized and fluorescent poly(alkyl cyanoacrylate) nanoparticles (NPs) and their evaluation for the targeting of the $A\beta_{1-42}$ peptide are reported. The synthetic strategy relied on the design of amphiphilic copolymers by tandem Knoevenagel–Michael addition of cyanoacetate derivatives, followed by their self-assembly in aqueous solutions to give the corresponding NPs. Different cyanoacetates were used: (i) hexadecyl cyanoacetate (HDCA) to form the hydrophobic core of the NPs; (ii) rhodamine B cyanoacetate (RCA) for fluorescent purposes; (iii) methoxypoly(ethylene glycol) cyanoacetate (MePEGCA) for stealth properties and (iv) selegiline-poly(ethylene glycol) cyanoacetate (SelPEGCA) to obtain the desired functionality. Two different amphiphilic copolymers were synthesized, a selegiline-containing copolymer, P(MePEGCA-*co*-SelPEGCA-*co*-HDCA), and a rhodamine-labelled counterpart, P(MePEGCA-*co*-RCA-*co*-HDCA), further blended at variable ratios to tune the amount of selegiline moieties displayed at the surface of the NPs.

Optimal formulations involving the different amphiphilic copolymers were determined by the study of the NP colloidal characteristics. Interestingly, it was shown that the zeta potential value of the selegiline-functionalized nanoparticles dramatically decreased, thus emphasizing a significant modification in the surface charge of the nanoparticles. Capillary electrophoresis has then been used to test the ability of the selegiline-functionalized NPs to interact with the $A\beta_{1-42}$ peptide. In comparison with non functionalized NPs, no increase of the interaction between these functionalized NPs and the monomeric form of the $A\beta_{1-42}$ peptide was observed, thus highlighting the lack of availability of the ligand at the surface of the nanoparticles. A mechanism explaining this result has been proposed and was mainly based on the burial of the hydrophobic selegiline ligand within the nanoparticles core.

1. Introduction

Alzheimer's disease (AD) is a severe neurodegenerative illness affecting more and more aging population over the world. AD represents the most common cause of dementia and is characterized by a progressive, but irreversible deterioration of cognitive functions and a loss of memory (Querfurth and LaFerla, 2010). Although the mechanisms leading to these dysfunctions are still unclear and under debate (Aliev et al., 2004; de la Torre, 2004; Korolainen et al., 2010), the disease is physiologically characterized by two main pathological features. These hallmarks are: (i) the intracellular accumulation of the hyperphosphorylated tau protein in the neurons and (ii) the progressive production and aggregation of β-amyloid peptide (Aβ) (Aguzzi and O'Connor, 2010; Panza et al., 2009), the latter being considered as the main cause of AD (Gralle et al., 2009). Neurons produce Aβ peptides with a variable number of amino-acids and the Aβ peptide 1–42 ($A\beta_{1-42}$) is believed to be the most representative and the most toxic species in AD physiopathology due to its high tendency to spontaneously self-aggregate (Chow et al., 2010; García-Matas et al., 2010).

In the last decades, the pharmaceutical companies have only attempted to combat clinical manifestations of AD. In particular, acetylcholinesterase (AchE) inhibitors (Birks et al., 2009; Munoz-

* Corresponding author. Tel.: +33 1 46 83 58 53; fax: +33 1 46 83 59 46.
** Corresponding author. Tel.: +33 1 46 83 58 12; fax: +33 1 46 83 59 46.
E-mail addresses: julien.nicolas@u-psud.fr (J. Nicolas), karine.andrieux@u-psud.fr, karine.andrieux@cep.u-psud.fr (K. Andrieux).
[1] These authors contributed equally to this work.

0378-5173/$ – see front matter © 2011 Elsevier B.V. All rights reserved.
doi:10.1016/j.ijpharm.2011.01.015

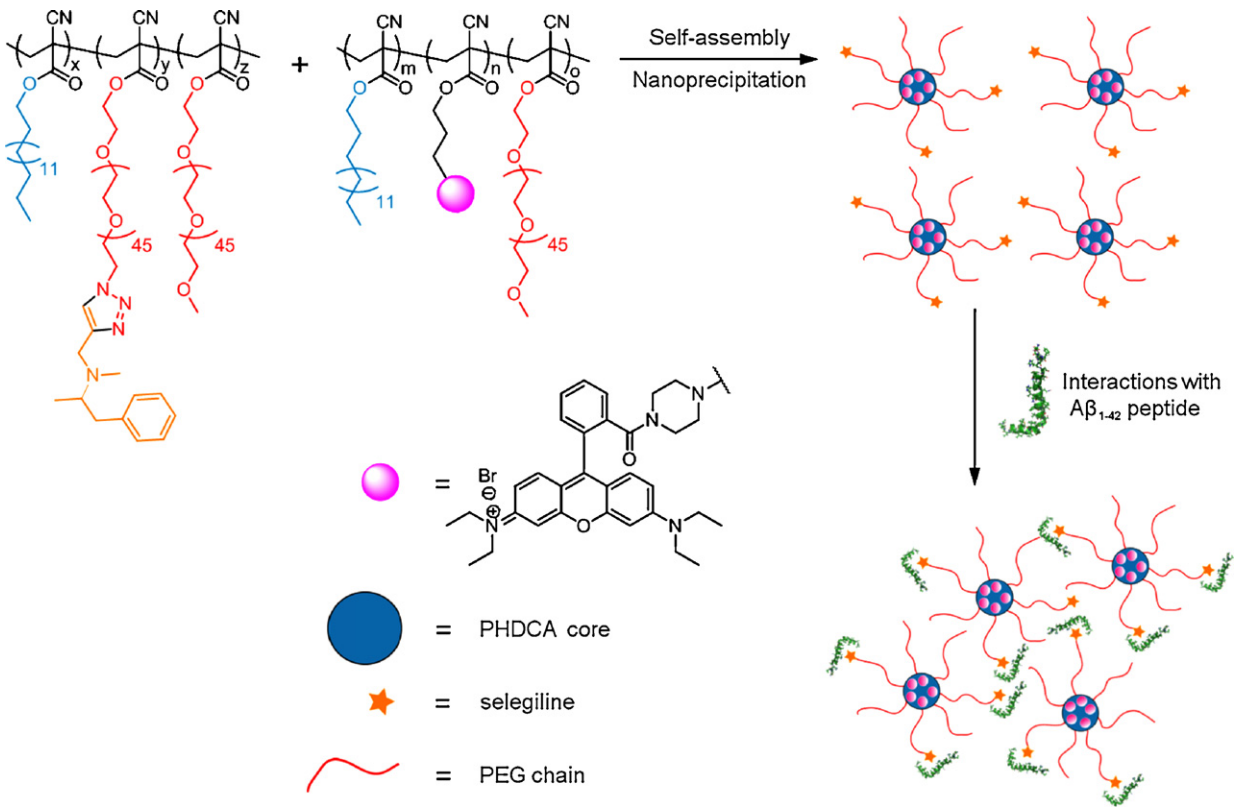

Fig. 1. General approach for the synthesis of selegiline-functionalized, PEGylated poly(alkyl cyanoacrylate) nanoparticles and their possible interaction with the HiLyte Fluor™ 488 labelled amyloid-β 1–42 ($A\beta_{1-42}$) peptide.

Torrero, 2008; Sugimoto et al., 1995) and *N*-methyl-D-aspartate (NMDA) receptor antagonists (Kemp and McKernan, 2002; Parsons et al., 1999; Reisberg et al., 2003) have been widely used but without significant success. Unfortunately, no efficient treatment aiming at the eradication of AD has been proposed so far.

Recently, different studies promoted the utilization of small aromatic molecules for targeting the $A\beta_{1-42}$ peptide, such as curcumine (Garcia-Alloza et al., 2007; Lim et al., 2001; Ono et al., 2004) and its derivatives (Narlawar et al., 2008), Thioflavine T (Xie et al., 2006), Congo red (Carter and Chou, 1998; Lorenzo and Yankner, 1994; Virginia, 2002) and their analogues such as Chrysamine G (Klunk et al., 1998; Lee, 2002; Virginia, 2002) and X34 (Christopher et al., 2001; Styren et al., 2000). These molecules have shown a certain efficiency to hinder, or even to stop, the oligomerization of the $A\beta_{1-42}$ peptide and thus the production of oligomers and/or fibrils, which are commonly considered as the toxic species for neuronal cells. These ligands have also been extensively used as tracers of the presence of senile plaques in the brain due to their fluorescent properties. Moreover, they can be modified with radiolabelled elements for diagnostic purposes (Dezutter et al., 1999a, 1999b; Nordberg, 2004; Wang et al., 2002, 2004). Unfortunately, these compounds do not overpass the blood–brain barrier (BBB). To circumvent this crucial problem, researchers have developed three main strategies: (i) the chemical modification of ligands to make them able to cross the BBB, (ii) their encapsulation into nanoparticles (NPs) and (iii) their ligation to NPs (Narlawar et al., 2008; Sun et al., 2010).

Among the pool of efficient ligands discovered so far, we have focused our attention on selegiline, an aromatic molecule that has been employed to slow down the progression of the Parkinson's disease (Tetrud and Langston, 1989), but that has been more importantly used as monoamine oxidase-B inhibitor for the treatment of AD (Sano et al., 1997; Tom, 2000; Wilcock et al., 2002). Selegiline also exhibited a certain affinity for the $A\beta_{1-42}$ peptide (Re et al., 2010). In this study, we presented the synthesis of selegiline-functionalized and fluorescent poly(alkyl cyanoacrylate) nanoparticles for $A\beta_{1-42}$ peptide targeting and anti-fibrillogenesis purposes. By capturing monomeric peptide at the surface of these nanoparticles, we aim to inhibit its fibrillogenesis. The synthesis strategy relied on the dual modification of poly[methoxypoly(ethylene glycol) cyanoacrylate-*co*-poly(hexadecyl cyanoacrylate)] (P(MePEGCA-*co*-HDCA)) copolymers (Nicolas and Couvreur, 2009; Peracchia et al., 1999) to introduce: (i) selegiline moieties at the extremity of PEG chains and (ii) rhodamine B probes within the copolymer structure. The P(MePEGCA-*co*-HDCA) copolymer scaffold has been selected due to its successful ability to cross the BBB (Calvo et al., 2001; Garcia-Garcia et al., 2005a, 2005b). Moreover, we took advantage of a recent study that demonstrated the efficient derivatization of such copolymers with azido-functional groups allowing subsequent reaction with alkyne-containing ligands through copper-catalyzed azide–alkyne cycloaddition (CuAAC) (Nicolas et al., 2008). Functionalization was undertaken with selegiline by CuAAC *via* its native alkyne group. NPs were obtained from the self-assembly of different ratios of selegiline-functionalized and rhodamine B-tagged copolymers in order to tune the amount of selegiline moieties displayed at their surface (Fig. 1). The resulting functionalized nanoparticles, obtained by the nanoprecipitation technique, were characterized by dynamic light scattering (DLS) and zeta potential (ζ) measurements. Finally, we used capillary electrophoresis (CE) to monitor the interaction of the selegiline-functionalized NPs with the $A\beta_{1-42}$ peptide (Brambilla et al., 2010b).

2. Materials and methods

2.1. Materials

Azidopoly(ethylene glycol) cyanoacetate (N_3PEGCA, M_n = 2 kDa), methoxypoly(ethylene glycol) cyanoacetate (MePEGCA, M_n = 2 kDa) and hexadecyl cyanoacetate (HDCA) were obtained from already published synthetic procedures (Nicolas et al., 2008). Poly[hexadecyl cyanoacrylate-*co*-rhodamine B cyanoacrylate-*co*-methoxypoly(ethylene glycol) cyanoacrylate] (P(HDCA-*co*-RCA-*co*-MePEGCA), **C1**) copolymer containing 5% rhodamine cyanoacetate (with respect to HDCA monomer) and poly[hexadecyl cyanoacrylate-*co*-azidopoly(ethylene glycol) cyanoacrylate] P(HDCA-*co*-N_3PEGCA) copolymers were obtained by tandem Knoevenagel–Michael addition of cyanoacetate (Brambilla et al., 2010a; Nicolas et al., 2008). NaH_2PO_4 (>99%) was purchased from Merck & Co (Fontenay-sous-Bois, France). Na_2HPO_4 (>98%) was obtained from Prolabo (Strasbourg, France). Pluronic F-68 (99%), sodium carbonate (Na_2CO_3, BioUltra, minimum 99.5%) and sodium dodecyl sulfate (SDS, 99%), R-(−)-Deprenyl hydrochloride (selegiline, ≥98%), *N*-dicyclohexylcarbodiimide (DCC, Fluka, ≥99% GC), 4-dimethylaminopyridine (DMAP, 99%), formaldehyde solution (37 wt.% in water, contains 10–15% methanol as stabilizer), pyrrolidine (99% GC, T), copper sulfate pentahydrate ($CuSO_4{\cdot}5H_2O$, ≥98%), (+)-sodium L-ascorbate (crystalline, 98%), ethylenediaminetetraacetic acid tetrasodium salt hydrate (EDTA, practical grade ~95%) were purchased from Sigma–Aldrich (St. Quentin Fallavier, France). Sodium hydroxide (NaOH) solution (1 M) was obtained from VWR (Fontenay-sous-Bois, France). All solvents were purchased at the highest grade from Carlo Erba (Val de Reuil, France). Deuterated chloroform ($CDCl_3$, ≥99.8 atom% D) and dimethyl sulfoxide (DMSO-d_6, ≥99.8 atom% D) were obtained from Sigma–Aldrich and used as received.

Lyophilized HiLyte Fluor™ 488 labelled amyloid-β 1–42 ($A\beta_{1-42}$) peptide was provided by ANASPEC (Le Perray en Yvelines, France). Spectra/Por dialysis bags (2 kDa molecular weight cut off) were purchased from Spectrum Laboratories Inc. and used after washing in deionized water for 1 h.

2.2. Analytical techniques

2.2.1. ^{1}H NMR spectroscopy

All ^{1}H NMR spectra were performed in deuterated solvents ($CDCl_3$ or d_6-DMSO) at ambient temperature on a Bruker Avance 300 MHz spectrometer.

2.2.2. Mean average diameter and zeta potential measurements

Nanoparticles average diameter (D_z) was measured by dynamic light scattering (DLS) with a Nano ZS from Malvern (173° scattering angle) at a temperature of 25 °C. Colloidal stability was evaluated as a function of time in different buffers (cell culture medium, phosphate buffer saline) at 25 °C. The zeta potential (ζ) was calculated with the same apparatus from the electrophoretic mobility (u) using the Smoluchowsky relationship $\zeta = \eta u/\varepsilon f(\kappa a)$, where it is assumed that $\kappa a \gg 1$, where η is the solution viscosity, ε is the dielectric constant of the medium, and κ and a are the Debye–Hückel parameter and the particle radius, respectively, $f(\kappa a)$ is the Henry's function and its value is 1.5 (Smoluchowski approximation) when the electrophoretic determinations of zeta potential are made in aqueous media and moderate electrolyte concentration. Zeta-potential measurements of nanoparticle dilute aqueous solutions were carried out at 25 °C in 10^{-3} M KCl.

2.2.3. Capillary electrophoresis

Capillary electrophoresis (CE) was performed on a PA 800 instrument (Beckman Coulter, Roissy, France) using uncoated silica capillaries (Phymep, Paris) with an internal diameter of 50 μm and 50 cm total length (40 cm effective length was employed for the separation). All buffers were prepared with deionized water and were filtered through a 0.22 μm membrane (VWR) before use. Prior analysis, the capillaries were preconditioned by the following rinsing sequence: 0.1 M NaOH for 5 min, 1 M NaOH for 5 min and then deionized water for 5 min. The in-between run rinsing cycles were carried out by pumping sequentially through the capillary: water for 5 min, 50 mM SDS for 2 min, to inhibit the aggregation and subsequent peptide adsorption on the capillary wall, and 0.1 M NaOH for 5 min. The samples were introduced into the capillary by hydrodynamic injection under 3.4 kPa. The capillary was thermostated at 25 °C and the samples were maintained at 37 °C by the storage sample module of the PA 800 apparatus. The separations were carried out at 16 kV with positive polarity at the inlet using 80 mM phosphate buffer pH 7.4. The running electrolyte was renewed after each run. The fluorescent peptide was detected by a laser-induced fluorescence (LIF) detection system equipped with 3.5 mW argon-ion laser with a wavelength excitation of 488 nm, the emission being collected through a 520 nm band-pass filter. Peak areas were estimated using the 32 Karat™ software (Beckman Coulter). The results are expressed as the evolution of percentage of monomer peak area as a function of time (Brambilla et al., 2010b).

2.3. Synthesis of P(MePEGCA-co-SelPEGCA-co-HDCA) copolymers

2.3.1. Neutral form of selegiline

Selegiline·HCl (100 mg, 0.45 mmol) was dispersed in a 1 M Na_2CO_3 solution (5 mL, 5 mmol). The solution was vigorously stirred for 1 h and transferred into a separation funnel. Neutralized selegiline was extracted with diethylether (3× 15 mL). The joined organic fractions were dried over $MgSO_4$, filtered off and the solvent was removed under reduced pressure to give the desired product as a colourless oil in a quantitative yield. ^{1}H NMR (d_6-DMSO, 298 K) δ (ppm): 0.87 (d, 3H, J = 6.6 Hz), 2.27 (s, 3H), 2.90 (td, 2H, J = 4.1 and 12.6 Hz), 3.10 (t, 1H, J = 2.5 Hz), 3.35 (t, 2H, J = 2.45 Hz), 7.13–7.20 (m, 3H), 7.22–7.30 (m, 2H).

2.3.2. Selegiline-poly(ethylene glycol) (SelPEG)

Selegiline-poly(ethylene glycol) was obtained by click chemistry (Kolb et al., 2001). In a 10 mL round bottom flask, azidopoly(ethylene glycol) (200 mg, 0.1 mmol) and neutralized selegiline (37.5 mg, 0.2 mmol) were dissolved in 2 mL of a 1:1 ^{t}BuOH/deionized water mixture. The solution was bubbled for 10 min with nitrogen at room temperature. Then, $CuSO_4{\cdot}5H_2O$ (2.5 mg, 0.01 mmol) and (+)-sodium L-ascorbate (4.0 mg, 0.02 mmol) were dissolved in 1 mL of deionized water and the resulting solution was immediately added to the reaction mixture, followed by nitrogen bubbling for another 20 min and finally stirred overnight at room temperature under nitrogen atmosphere. ^{t}BuOH was then removed under reduced pressure and the aqueous solution was diluted with 1 mL of a 1 M EDTA aqueous solution and extensively dialyzed against deionized water using a 2 kDa dialysis bags. After dialysis, water was removed under reduced pressure and the product, dissolved in DCM, was dried over $MgSO_4$. After removal of the solvent, the pure product was obtained as a slightly brown powder with 75% yield. ^{1}H NMR (298 K, $CDCl_3$) δ (ppm): 1.13 (d, 3H, J = 5.5 Hz), 2.55 (br s, 3H), 3.35–3.94 (m, 188H), 4.20 (s, 2H), 4.57 (t, 2H, J = 5.1 Hz), 7.19–7.35 (m, 5H), 8.06 (s, 1H).

2.3.3. Synthesis of selegiline-poly(ethylene glycol) cyanoacetate (SelPEGCA)

In a 10 mL round bottom flask containing the selegiline-poly(ethylene glycol) (150 mg, 68 μmol) and cyanoacetic acid (11.5 mg, 136 μmol), were added 2 mL of DCM and 1 mL of ethylacetate. The resulting solution was cooled down with ice and placed under nitrogen atmosphere. DCC (21 mg, 102 μmol) and a catalytic amount of DMAP were dissolved in 1 mL of DCM and added dropwise. The reaction mixture was stirred at room temperature overnight under nitrogen atmosphere. After filtration to discard the insoluble dicyclohexylurea (DCU), the solvents were removed under reduced pressure and the resulting residue was dissolved in a minimum of DCM and precipitated in cold diethyl ether to give the pure product as a slightly brown powder with 86% yield. ^{1}H NMR (298 K, $CDCl_3$) δ (ppm): 1.15 (d, 3H, J = 5.5 Hz), 2.52 (br s, 3H), 3.52 (s, 2H), 3.35–3.94 (m, 188H), 4.19 (s, 2H), 4.35 (t, 2H, J = 4.7 Hz), 4.59 (t, 2H, J = 5.1 Hz), 7.19–7.35 (m, 5H), 8.06 (s, 1H).

2.3.4. Synthesis of selegiline-functionalized copolymer

The procedure for the synthesis of 10% selegiline-functionalized copolymer (P(MePEGCA-*co*-SelPEGCA-*co*-HDCA)) is as follows. In a 10 mL round bottom flask were introduced HDCA (120 mg, 0.38 mmol), MePEGCA (180 mg, 0.864 mmol) and SelPEGCA (22 mg, 0.096 mmol) in 2 mL of DCM and 1 mL of EtOH. To this solution were consecutively added dropwise formalin (0.2 mL, 4.43 mmol) and pyrrolidine (10 μL, 0.122 mmol). The reaction was stirred overnight under nitrogen atmosphere. The solvents were removed under reduced pressure and the residue was redissolved in DCM. The organic phase was washed with 3 portions of deionized water, once with 1 M HCl solution, once with brine and finally dried over $MgSO_4$. The solvent was removed under reduced pressure to afford the resulting copolymer as a slightly brown sticky solid (92% yield). ^{1}H NMR (298 K, $CDCl_3$, 300 MHz) δ (ppm): 0.81 (t, 12H, J = 6.6 Hz), 0.96–1.41 (m, 104H), 1.66 (m, 8H), 2.25–2.77 (br m, 8H), 3.30 (s, 2.7H), 3.33–3.84 (m, 188H), 4.19 (br s, 10H), 4.59 (t, 0.2H, J = 5.2 Hz), 7.11–7.29 (m, 0.5H), 8.04 (s, 0.1H).

2.4. Nanoparticle preparation

A typical procedure for the preparation of selegiline-functionalized nanoparticles (Table 1, **N6**) is as follows. 5 mg of 10% selegiline-functionalized P(MePEGCA-*co*-SelPEGCA-*co*-HDCA) copolymer and 5 mg of P(MePEGCA-*co*-RCA-*co*-HDCA) copolymer were dissolved in 2 mL of acetone. This solution was added dropwise to an aqueous solution of 0.5% (w/v) of Pluronic F-68 (4 mL) under vigorous stirring. Nanoparticle suspension formed immediately. Acetone was then removed under reduced pressure and the nanoparticles were purified by ultracentrifugation (150,000 × g, 1 h, 4 °C, Beckman Coulter, Inc.). The supernatant was discarded and the pellet was resuspended in the appropriate volume of deionized water to yield a 2.5 mg mL^{-1} nanoparticle suspension. The colloidal characteristics of the nanoparticles were then analyzed by DLS and zeta potential measurement.

2.5. Peptide sample preparation and storage

Lyophilized HiLyte Fluor^{TM} 488 labelled Aβ_{1-42} peptide was dissolved in 0.16% (w/v) of ammonium hydroxide aqueous solution to reach a concentration of 0.5 mg mL^{-1}. The peptide solution was then divided into aliquots, individually stored at −20 °C freshly thawed prior analysis.

2.6. Nanoparticle interaction with monomeric Aβ_{1-42}

To study the interaction between the monomeric form of the fluorescent Aβ_{1-42} peptide and the selegiline-functionalized nanoparticles, aliquots of HiLyte Fluor^{TM} 488 labelled Aβ_{1-42} peptide stock solutions were diluted in 20 mM phosphate buffer (NaH_2PO_4) pH 7.4 containing 20 μM of P(MePEGCA-*co*-RCA-*co*-HDCA) nanoparticles **N3** or **N8** to obtain a final peptide concentration of 5 μM. The samples were then incubated at 37 °C and analyzed by CE approximately every 2 h using LIF detection (Brambilla et al., 2010b).

3. Results and discussion

As previously mentioned, the "amyloid hypothesis" (*i.e.* the hypothesis that the amyloid fibrils formed by oligomerization of Aβ peptides and especially of the Aβ_{1-42} peptide are the major causes of the neuronal degeneration), is so far considered by researchers as the most probable cause of AD. Consequently, more and more research groups have focused their efforts on the inhibition of this fibrillogenesis with suitable compounds/ligands. Among these ligands, selegiline has been chosen due to its terminal alkyne functionality that allowed for further covalent linkage on azide-containing copolymers/nanoparticles *via* CuAAC reaction. The synthesis of selegiline-functionalized poly(alkyl cyanoacrylate) nanoparticles was therefore undertaken.

3.1. Synthesis and characterization of selegiline-functionalized copolymers

Prior functionalization of PEGCA with selegiline, its hydrochloric salt was turned into its neutral form using Na_2CO_3 in order to avoid any alteration of the copper catalyst involved in the CuAAC. Indeed, some preliminary studies (data not shown) yielded no coupling when selegiline, hydrochloric salt was used under standard click conditions. Neutral selegiline was obtained quantitatively as confirmed by ^{1}H NMR spectroscopy that displayed all protons accounting for the molecule (see Section 2).

We took advantage of a recent study which demonstrated the covalent linkage of model ligands, either at the surface of azido-functionalized nanoparticles or directly to the corresponding copolymer (Nicolas et al., 2008). However, in the present study, a slightly different approach was used whereby a functionalized poly(ethylene glycol) cyanoacetate was first prepared prior synthesis of the corresponding copolymer. Selegiline-poly(ethylene glycol) cyanoacetate (SelPEGCA) was copolymerized with HDCA and MePEGCA in the presence of ethanol, formalin and pyrrolidine to give the selegiline-functionalized P(MePEGCA-*co*-SelPEGCA-*co*-HDCA) copolymer. It was characterized by ^{1}H NMR spectroscopy which confirmed the presence of selegiline moieties within the copolymer structure, *via* its aromatic protons (see Section 2).

3.2. Formation and characterization of selegiline-functionalized nanoparticles

The ability of the selegiline-functionalized poly(alkyl cyanoacrylate) copolymers to form nanoparticles by self-assembly was assessed and the suspensions of nanoparticles were then characterized by DLS and zeta potential measurements as stability studies.

P(MePEGCA-*co*-SelPEGCA-*co*-HDCA) nanoparticles **N1** and **N2** containing respectively 10 or 50% SelPEGCA (with respect to the overall PEGCA content of the copolymer) were prepared by the nanoprecipitation technique. Their characterization revealed that nanoparticles **N2** obtained by including 50% SelPEGCA exhibited a poor colloidal stability. Indeed, several minutes after their formation, the average diameter dramatically increased from approximately 150 to 200 nm, together with an increase of the particle size distribution (PSD) from less than 0.2 to 0.4. The

Table 1
Compositions and initial colloidal properties of selegiline-functionalized poly(alkyl cyanoacrylate) nanoparticles.

Expt.	P(MePEGCA-*co*-SelPEGCA-*co*-HDCA) copolymer **C1**[a] (wt.%)	P(MePEGCA-*co*-RCA-*co*-HDCA) copolymer **C2** (wt.%)	SelPEGCA[b] (mol.%)	Average particle diameter[d] (D_z) (nm)	Particle size distribution[c,d]	Zeta potential[d] (ζ) (mV)
1 (**N8**)	90	10	9	93	0.16	9
2 (**N7**)	70	30	7	92	0.13	7.9
3 (**N6**)	50	50	5	96	0.16	−2.4
4 (**N5**)	10	90	1	104	0.18	−12.9
5 (**N4**)	5	95	0.5	110	0.14	−11.1
6 (**N3**)	2	98	0.2	113	0.18	−14.9

[a] Copolymer containing 10% SelPEGCA with respect to PEGCA overall content.
[b] With respect to PEGCA overall content.
[c] Given by the DLS apparatus.
[d] Values measured immediately after purification of the nanoparticles.

nanoparticles **N1** synthesized with only 10% SelPEGCA displayed a mean average diameter of around 100 nm (PSD ~ 0.2). But, within 2 days, their size also increased significantly together with an increase of their particle size distribution above 0.3. Even after some efforts to change the nanoprecipitation parameters (such as the organic phase/aqueous phase ratio or the percentage of Pluronic F-68 surfactant added to the aqueous solution), the poor P(MePEGCA-*co*-SelPEGCA-*co*-HDCA) nanoparticle stability remained unchanged. Therefore, a co-nanoprecipitation approach with P(MePEGCA-*co*-SelPEGCA-*co*-HDCA) (**C1**) and P(MePEGCA-*co*-RCA-*co*-HDCA) (**C2**) copolymers was investigated. Indeed, P(MePEGCA-*co*-RCA-*co*-HDCA) copolymer **C2** exhibited a great colloidal stability over time and a rather low zeta potential value (around -40.6 ± 0.3 mV) (Brambilla et al., 2010a). Variable blends of these two copolymers **C1** and **C2** were tested (see Table 1).

These new formulations of selegiline-functionalized nanoparticles **N3** to **N8**, incorporating from 0.2 to 9% selegiline PEGCA, respectively, were characterized by DLS and zeta potential measurement (Table 1). These nanoparticles displayed average diameters in the 90–120 nm range with narrow particle size distribution (PSD < 0.2), together with zeta potential values varying from 10 to −15 mV. It was observed that the more selegiline-functionalized copolymer incorporated in the formulation, the higher the zeta potential. This demonstrated the presence of the selegiline ligands at the surface of the nanoparticles, rendering their surface more positively charged than the non-functionalized ones. The NPs were then subjected to DLS measurements over a period of 8 days in deionized water at 25 °C (Fig. 2). It was shown that the mean average diameter remained rather stable (the variation observed for **N6** at day 7 should not be considered relevant).

However, as shown in Fig. 3, the zeta potential values of nanoparticles **N3**–**N8** dramatically decreased within 1 or 2 days, whereas it remained rather constant for rhodamine B-labelled P(MePEGCA-*co*-RCA-*co*-HDCA) NPs as previously published (Brambilla et al., 2010a). Indeed, an average drop of ~15 mV was observed, indicating a change in the physico-chemical properties at the surface of the nanoparticles. Following this marked decrease, the zeta potential remained stable, close to values usually observed for P(MePEGCA-*co*-RCA-*co*-HDCA) nanoparticles (Brambilla et al., 2010a).

The stability of these NPs was also assessed in phosphate buffer saline (pH 7.4) used in CE analysis and in cell culture medium. As observed in Fig. 4, the average diameter of the nanoparticles remained rather stable up to one week with a particle size distribution below 0.3 in both buffers. The decrease in zeta potential was observed in both media, still confirming the surface charge evolution of the nanoparticles with time (data not shown). However, this good stability of the average diameter for nanoparticles **N3**–**N8** in phosphate buffer allowed further studies of their interactions with the $A\beta_{1-42}$ peptide by CE.

3.3. Interaction of the nanoparticles with the $A\beta_{1-42}$ peptide

CE is an analytical technique that has been recently used for the screening and identification of efficient ligands towards their inhibition properties against $A\beta_{1-42}$ peptide aggregation (Colombo et al., 2009; Kato et al., 2007; Sabella et al., 2004). Thereby, we recently developed an innovative protocol based on capillary electrophoresis coupled to laser-induced fluorescence (CE-LIF) detection to monitor the interactions of P(MePEGCA-*co*-RCA-*co*-HDCA) nanoparticles with the $A\beta_{1-42}$ peptide (Brambilla et al., 2010b). Interestingly, it was demonstrated that the P(MePEGCA-*co*-

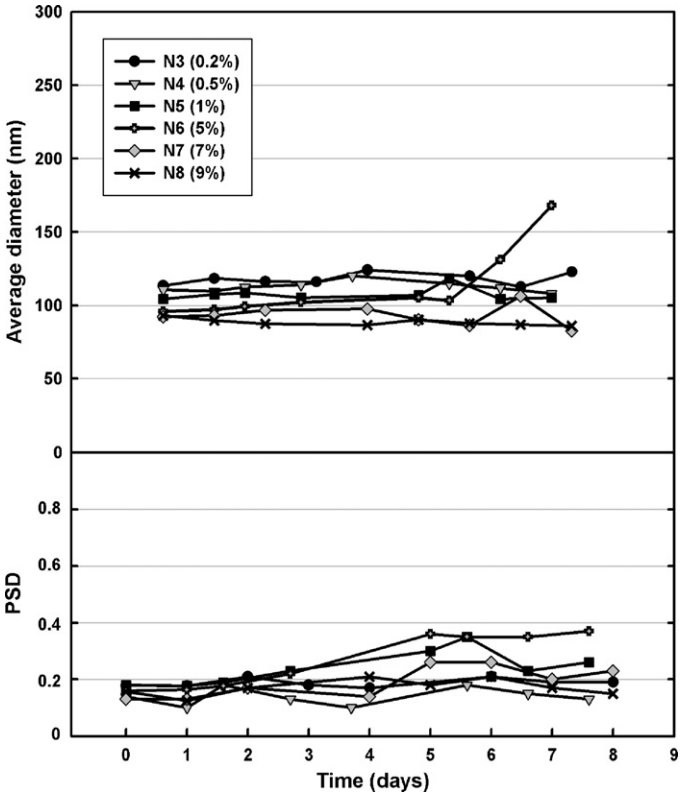

Fig. 2. Evolution with time of the average diameter and of the particle size distribution (PSD) in deionized water at 25 °C of the selegiline-functionalized nanoparticles as a function of the selegiline content within the copolymer mixture: (●) **N3** (0.2%); (▽) **N4** (0.5%); ( ) **N5** (1%); (+) **N6** (5%); ( ) **N7** (7%); (×) **N8** (9%).

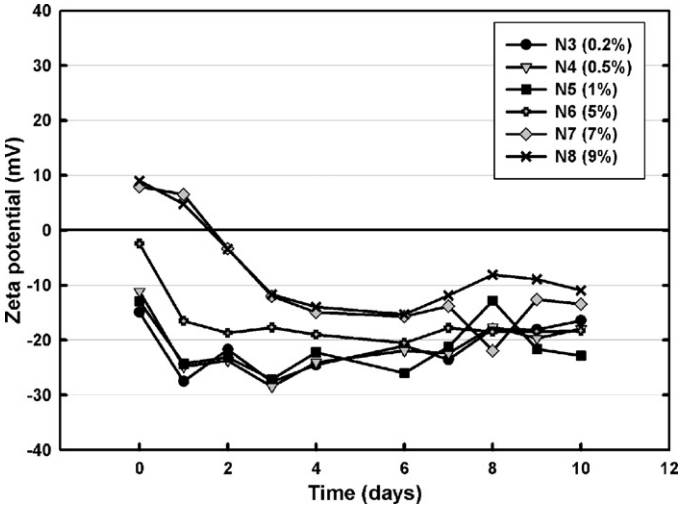

Fig. 3. Evolution with time of the zeta-potential values in deionized water at 25 °C of selegiline-functionalized nanoparticles as a function of the selegiline content within the copolymer mixture: (●) **N3** (0.2%); (▽) **N4** (0.5%); ( ) **N5** (1%); (+) **N6** (5%); ( ) **N7** (7%); (×) **N8** (9%).

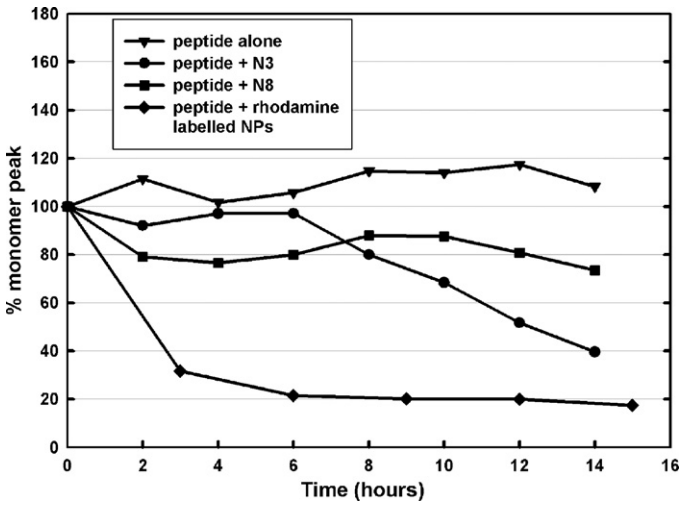

Fig. 5. Comparative evolution of area under curve of HiLyte Fluor™ 488 labelled $A\beta_{1-42}$ peptide monomeric peak alone (blank, ▼), and in presence of non-functionalized ( ) or selegiline-functionalized nanoparticles **N3** (●) and **N8** ( ).

RCA-*co*-HDCA) nanoparticles were able to bind the $A\beta_{1-42}$ peptide under its so-called "monomeric" form. We claimed that this protocol could be relevant to screen NPs for $A\beta_{1-42}$ targeting and to discover suitable candidates.

Herein, we investigated the interaction of such a functionalization of a similar polymeric scaffold with selegiline, with the $A\beta_{1-42}$ peptide using CE coupled to LIF detection. Samples of fluorescently tagged $A\beta_{1-42}$ peptide incubated with nanoparticles **N3** and **N8** were analyzed every 2 h using a LIF detection system that allowed monitoring the relative concentration of the peptide. P(MePEGCA-*co*-RCA-*co*-HDCA) nanoparticles dramatically decrease the area under the curve (AUC) of the $A\beta_{1-42}$ peptide monomeric peak (from 100 to 20% after 6 h) whereas this value remained unchanged in the absence of any polymeric nanocarrier (control experiment, AUC ~ 100% after 14 h) as observed in Fig. 5. These data combined with other results have been related to the adsorption of the peptide at the surface of P(MePEGCA-*co*-RCA-*co*-HDCA) nanoparticles (Brambilla et al., 2010b). Regarding Aβ peptide affinity, the roles of PEG and rhodamine are still unclear but are under investigation.

However, under identical experimental conditions, no important decrease of the $A\beta_{1-42}$ peptide monomer peak was observed in the case of selegiline-functionalized nanoparticles (**N3** and **N8**) when compared to their non-functionalized counterparts (Fig. 5). The effect was even lower, which confirmed an important evolution of the positioning of the ligand at the surface of

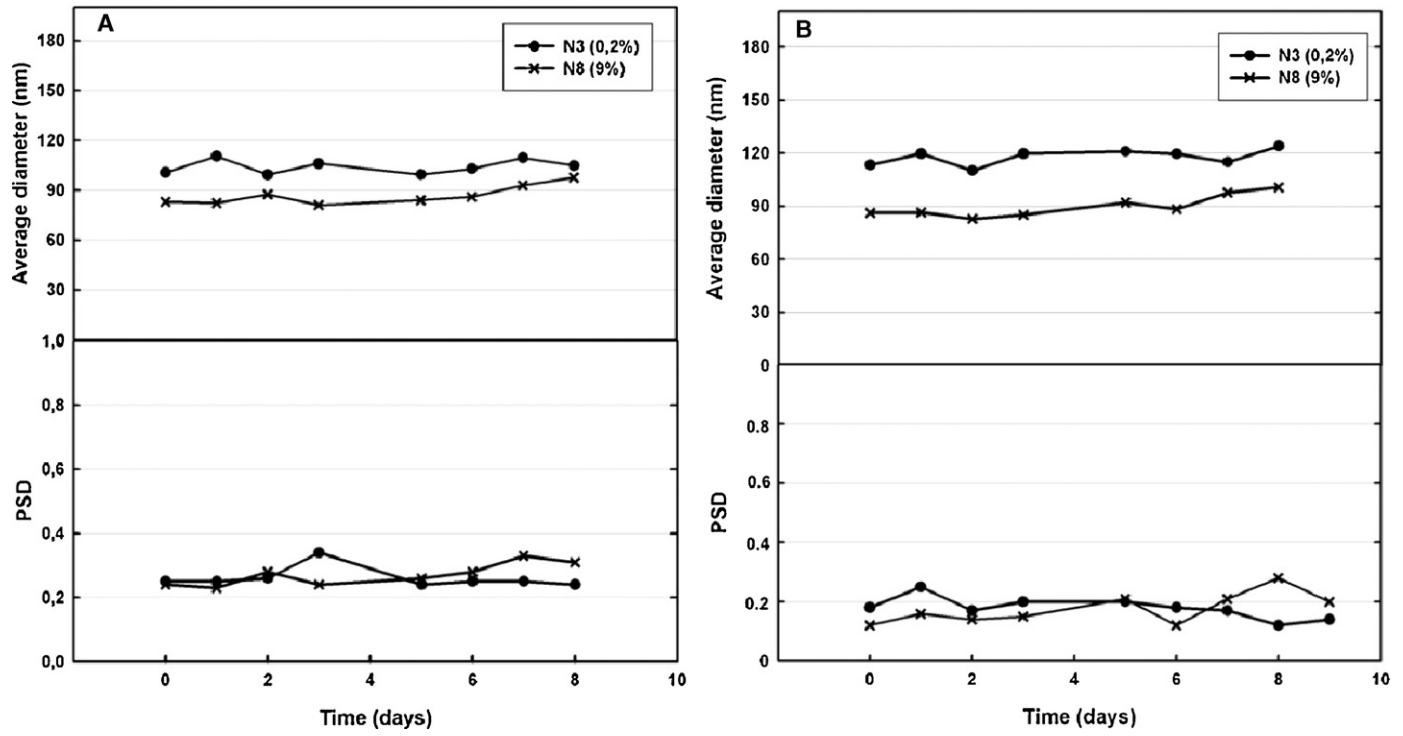

Fig. 4. Evolution of the average diameter and of the particle size distribution of selegiline-functionalized nanoparticles **N3** (●, 0.2% SelPEGCA) and **N8** (×, 9% SelPEGCA) at 25 °C in (A) cell culture medium and in (B) phosphate buffer saline pH 7.4 as a function of time.

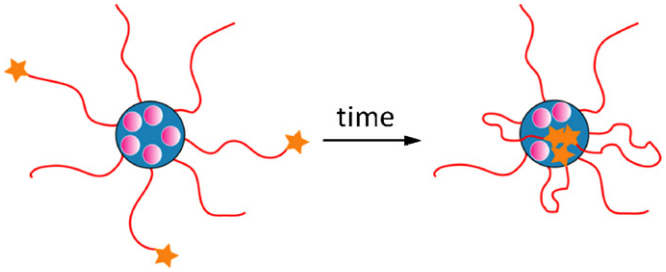

Fig. 6. Schematic representation describing the rearrangement of the seligiline ligands at the surface of the seligiline-functionalized nanoparticles **N3**–**N8**.

the P(MePEGCA-*co*-SelPEGCA-*co*-HDCA) nanoparticles. This inefficiency of selegiline-functionalized nanoparticles towards binding to the $A\beta_{1-42}$ peptide clearly demonstrated that the ligand was not well exposed and probably inaccessible for efficient interaction with $A\beta_{1-42}$ peptide which thus confirmed the hypothesis postulated earlier in this study.

Indeed, taken together with previous zeta potential measurements, these data indicate that, after a certain time, selegiline ligands which were initially exposed at the surface of the nanoparticles became not accessible anymore, likely due to rearrangement of the SelPEG chains. The hydrophobic nature of selegiline and/or possible hydrophobic interaction between selegiline moieties could conduct to PEG loops with selegiline extremities, either buried in the hydrophobic PHDCA core and/or stuck to each other by hydrophobic interactions (Fig. 6). This would conduct to a drastic change in the linear PEG density at the surface of the NPs, which is believed to be an important parameter regarding their binding to the $A\beta_{1-42}$ peptide (Brambilla et al., 2010b). This may certainly explain why selegiline-functionalized NPs exhibited less binding activity towards $A\beta_{1-42}$ peptide than non-functionalized, PEGylated NPs. In addition, the higher the selegiline amount in the NPs, the lower the binding efficiency towards the $A\beta_{1-42}$ peptide which is in good agreement with the expected decrease of the linear PEG chain density (in contrast to PEG loops) at the surface of the NPs for higher selegiline content (Fig. 6). The activity of nanoparticles **N8** is negligible if one considers the dramatic decrease of the Aβ monomer peak (within 3 h) in the case of non-functionalized NPs. This weak activity is probably more related to remaining MePEG chains at the surface of the NPs than to selegiline-PEG chains. We believe that if there were some specific interactions in-between the peptide and the exposed ligand, the variation of the peptide monomer peak would have been more intense.

4. Conclusion

This study investigated the potential binding activity of polymeric selegiline-functionalized, PEGylated poly(alkyl cyanoacrylate) nanoparticles to the $A\beta_{1-42}$ peptide, a biomarker of the Alzheimer's disease. Whereas a poor colloidal stability was obtained with the pure selegiline-functionalized copolymer, best stability conditions were obtained after simultaneous nanoprecipitation of this polymer with the rhodamine-labelled, PEGylated poly(alkyl cyanoacrylate) copolymer species in variable ratios. It allowed the amount of selegiline moieties initially displayed at the surface of the NPs to be finely tuned. Although the size of the selegiline-functionalized NPs remained constant with time, the value of the zeta potential drastically decreased. This was confirmed by capillary electrophoresis which showed a lower interaction of selegiline decorated nanoparticles towards $A\beta_{1-42}$ comparatively to the non-functionalized nanoparticles. A possible explanation was proposed and relied on a rearrangement of functionalized selegiline chains at the surface of the NPs leading to their complete inaccessibility towards $A\beta_{1-42}$. More importantly, this study points out the importance of the hydrophobicity/hydrophilicity of the selected ligand displayed at the surface of polymeric NPs.

Acknowledgments

The research leading to these results has received funding from the European Community's Seventh Framework Programme (FP7/2007-2013) under agreement no. 212043. The CNRS and the French Ministry of Research are also warmly acknowledged for financial support.

References

Aguzzi, A., O'Connor, T., 2010. Protein aggregation diseases: pathogenicity and therapeutic perspectives. Nat. Rev. Drug Discov. 9, 237–248.
Aliev, G., Smith, M.A., de la Torre, J.C., Perry, G., 2004. Mitochondria as a primary target for vascular hypoperfusion and oxidative stress in Alzheimer's disease. Mitochondrion 4, 649–663.
Birks, J., Grimley Evans, J., Iakovidou, V., Tsolaki, M., Holt, F.E., 2009. Rivastigmine for Alzheimer's disease. Cochrane Database Syst. Rev., CD001191.
Brambilla, D., Nicolas, J., Le Droumaguet, B., Andrieux, K., Marsaud, V., Couraud, P.-O., Couvreur, P., 2010a. Design of fluorescently tagged poly(alkyl cyanoacrylate) nanoparticles for human brain endothelial cell imaging. Chem. Commun. 46, 2602–2604.
Brambilla, D., Verpillot, R., Taverna, M., De Kimpe, L., Le Droumaguet, B., Nicolas, J., Mantegazza, F., Canovi, M., Gobbi, M., Salmona, M., Nicolas, V., Scheper, W., Couvreur, P., Andrieux, K., 2010b. Capillary electrophoresis with laser-induced fluorescence detection (CE-LIF) as a new protocol to monitor interaction between nanoparticles and the amyloid-β peptide. Anal. Chem. 82, 10083–10089.
Calvo, P., Gouritin, B., Chacun, H., Desmaële, D., D'Angelo, J., Noel, J.-P., Georgin, D., Fattal, E., Andreux, J.P., Couvreur, P., 2001. Long-circulating PEGylated polycyanoacrylate nanoparticles as new drug carrier for brain delivery. Pharm. Res. 18, 1157–1166.
Carter, D.B., Chou, K.C., 1998. A model for structure-dependent binding of Congo red to Alzheimer β-amyloid fibrils. Neurobiol. Aging 19, 37–40.
Chow, V., Mattson, M., Wong, P., Gleichmann, M., 2010. An overview of APP processing enzymes and products. Neuromol. Med. 12, 1–12.
Christopher, D.L., Carolyn, J.J., Virginia, F., Marie-Christine, P., David, H.H., Scot, S., Chester, A.M., William, E.K., 2001. Visualization of fibrillar amyloid deposits in living, transgenic Caenorhabditis elegans animals using the sensitive amyloid dye, X-34. Neurobiol. Aging 22, 217–226.
Colombo, R., Carotti, A., Catto, M., Racchi, M., Lanni, C., Verga, L., Caccialanza, G., De Lorenzi, E., 2009. CE can identify small molecules that selectively target soluble oligomers of amyloid β protein and display antifibrillogenic activity. Electrophoresis 30, 1418–1429.
de la Torre, J.C., 2004. Is Alzheimer's disease a neurodegenerative or a vascular disorder? Data, dogma, and dialectics. Lancet Neurol. 3, 184–190.
Dezutter, N.A., de Groot, T.J., Busson, R.H., Janssen, G.A., Verbruggen, A.M., 1999a. Preparation of ^{99m}Tc-N_2S_2 conjugates of Chrysamine G, potential probes for the beta-amyloid protein of Alzheimer's disease. J. Labelled Compd. Radiopharm. 42, 309–324.
Dezutter, N.A., Dom, R.J., de Groot, T.J., Bormans, G.M., Verbruggen, A.M., 1999b. ^{99m}Tc-MAMA-Chrysamine G, a probe for beta-amyloid protein of Alzheimer's disease. Eur. J. Nucl. Med. Mol. Imaging 26, 1392–1399.
Garcia-Alloza, M., Borrelli, L.A., Rozkalne, A., Hyman, B.T., Bacskai, B.J., 2007. Curcumin labels amyloid pathology in vivo, disrupts existing plaques, and partially restores distorted neurites in an Alzheimer mouse model. J. Neurochem. 102, 1095–1104.
Garcia-Garcia, E., Andrieux, K., Gil, S., Couvreur, P., 2005a. Colloidal carriers and blood–brain barrier (BBB) translocation: a way to deliver drugs to the brain? Int. J. Pharm. 298, 274–292.
Garcia-Garcia, E., Gil, S., Andrieux, K., Desmaële, D., Nicolas, V., Taran, F., Georgin, D., Andreux, J., Roux, F., Couvreur, P., 2005b. A relevant in vitro rat model for the evaluation of blood–brain barrier translocation of nanoparticles. Cell. Mol. Life Sci. 62, 1400–1408.
García-Matas, S., de Vera, N., Aznar, A.O., Marimon, J.M., Adell, A., Planas, A.M., Cristòfol, R., Sanfeliu, C., 2010. In vitro and in vivo activation of astrocytes by amyloid-β is potentiated by pro-oxidant agents. J. Alzheimer's Dis. 20, 229–245.
Gralle, M., Botelho, M.G., Wouters, F.S., 2009. Neuroprotective secreted amyloid precursor protein acts by disrupting amyloid precursor protein dimers. J. Biol. Chem. 284, 15016–15025.
Kato, M., Kinoshita, H., Enokita, M., Hori, Y., Hashimoto, T., Iwatsubo, T., Toyo'oka, T., 2007. Analytical method for β-amyloid fibrils using CE-laser induced fluorescence and its application to screening for inhibitors of β-amyloid protein aggregation. Anal. Chem. 79, 4887–4891.
Kemp, J.A., McKernan, R.M., 2002. NMDA receptor pathways as drug targets. Nat. Neurosci. 5, 1039–1042.

Klunk, W.E., Debnath, M.L., Koros, A.M.C., Pettegrew, J.W., 1998. Chrysamine-G, a lipophilic analogue of Congo red, inhibits Aβ-induced toxicity in PC12 cells. Life Sci. 63, 1807–1814.
Kolb, H.C., Finn, M.G., Sharpless, K.B., 2001. Click chemistry: diverse chemical function from a few good reactions. Angew. Chem. Int. Ed. 40, 2004–2021.
Korolainen, M.A., Nyman, T.A., Aittokallio, T., Pirttila, T., 2010. An update on clinical proteomics in Alzheimer's research. J. Neurochem. 112, 1386–1414.
Lee, V.M.Y., 2002. Amyloid binding ligands as Alzheimer's disease therapies. Neurobiol. Aging 23, 1039–1042.
Lim, G.P., Chu, T., Yang, F., Beech, W., Frautschy, S.A., Cole, G.M., 2001. The curry spice curcumin reduces oxidative damage and amyloid pathology in an Alzheimer transgenic mouse. J. Neurosci. 21, 8370–8377.
Lorenzo, A., Yankner, B.A., 1994. Beta-amyloid neurotoxicity requires fibril formation and is inhibited by Congo red. Proc. Natl. Acad. Sci. U.S.A. 91, 12243–12247.
Munoz-Torrero, D., 2008. Acetylcholinesterase inhibitors as disease-modifying therapies for Alzheimer's disease. Curr. Med. Chem. 15, 2433–2455.
Narlawar, R., Pickhardt, M., Leuchtenberger, S., Baumann, K., Krause, S., Dyrks, T., Weggen, S., Mandelkow, E., Schmidt, B., 2008. Curcumin-derived pyrazoles and isoxazoles: Swiss army knives or blunt tools for Alzheimer's disease? ChemMedChem 3, 165–172.
Nicolas, J., Bensaid, F., Desmaele, D., Grogna, M., Detrembleur, C., Andrieux, K., Couvreur, P., 2008. Synthesis of highly functionalized poly(alkyl cyanoacrylate) nanoparticles by means of click chemistry. Macromolecules 41, 8418–8428.
Nicolas, J., Couvreur, P., 2009. Synthesis of poly(alkyl cyanoacrylate)-based colloidal nanomedicines. Wiley Interdiscipl. Rev.: Nanomed. Nanobiotechnol. 1, 111–127.
Nordberg, A., 2004. PET imaging of amyloid in Alzheimer's disease. Lancet Neurol. 3, 519–527.
Ono, K., Hasegawa, K., Naiki, H., Yamada, M., 2004. Curcumin has potent anti-amyloidogenic effects for Alzheimer's β-amyloid fibrils in vitro. J. Neurosci. Res. 75, 742–750.
Panza, F., Solfrizzi, V., Frisardi, V., Imbimbo, B.P., Capurso, C., D'Introno, A., Colacicco, A.M., Seripa, D., Vendemiale, G., Capurso, A., Pilotto, A., 2009. Beyond the neurotransmitter-focused approach in treating Alzheimer's disease: drugs targeting beta-amyloid and tau protein. Aging Clin. Exp. Res. 21, 386–406.
Parsons, C.G., Danysz, W., Quack, G., 1999. Memantine is a clinically well tolerated N-methyl-D-aspartate (NMDA) receptor antagonist—a review of preclinical data. Neuropharmacology 38, 735–767.
Peracchia, M.T., Fattal, E., Desmaële, D., Besnard, M., Noël, J.P., Gomis, J.M., Appel, M., d'Angelo, J., Couvreur, P., 1999. Stealth® PEGylated polycyanoacrylate nanoparticles for intravenous administration and splenic targeting. J. Controlled Release 60, 121–128.
Querfurth, H.W., LaFerla, F.M., 2010. Alzheimer's disease. N. Engl. J. Med. 362, 329–344.
Re, F., Airoldi, C., Zona, C., Masserini, M., Ferla, B.L., Quattrocchi, N., Nicotra, F., 2010. Beta amyloid aggregation inhibitors: small molecules as candidate drugs for therapy of Alzheimers disease. Curr. Med. Chem. 17, 2990–3006.
Reisberg, B., Doody, R., Stoffler, A., Schmitt, F., Ferris, S., Mobius, H.J., 2003. Memantine in moderate-to-severe Alzheimer's disease. N. Engl. J. Med. 348, 1333–1341.
Sabella, S., Quaglia, M., Lanni, C., Racchi, M., Govoni, S., Caccialanza, G., Calligaro, A., Bellotti, V., De Lorenzi, E., 2004. Capillary electrophoresis studies on the aggregation process of β-amyloid 1–42 and 1–40 peptides. Electrophoresis 25, 3186–3194.
Sano, M., Ernesto, C., Thomas, R.G., Klauber, M.R., Schafer, K., Grundman, M., Woodbury, P., Growdon, J., Cotman, C.W., Pfeiffer, E., Schneider, L.S., Thal, L.J., 1997. A controlled trial of selegiline, alpha-tocopherol, or both as treatment for Alzheimer's disease. N. Eng. J. Med. 336, 1216–1222.
Styren, S.D., Hamilton, R.L., Styren, G.C., Klunk, W.E., 2000. X-34, a fluorescent derivative of Congo red: a novel histochemical stain for Alzheimer's disease pathology. J. Histochem. Cytochem. 48, 1223–1232.
Sugimoto, H., Iimura, Y., Yamanishi, Y., Yamatsu, K., 1995. Synthesis and structure–activity relationships of acetylcholinesterase inhibitors: 1-benzyl-4-[(5,6-dimethoxy-1-oxoindan-2-yl)methyl]piperidine hydrochloride and related compounds. J. Med. Chem. 38, 4821–4829.
Sun, M., Gao, Y., Guo, C., Cao, F., Song, Z., Xi, Y., Yu, A., Li, A., Zhai, G., 2010. Enhancement of transport of curcumin to brain in mice by poly(n-butylcyanoacrylate) nanoparticle. J. Nanopart. Res., 1–12.
Tetrud, J., Langston, J., 1989. The effect of deprenyl (selegiline) on the natural history of Parkinson's disease. Science 245, 519–522.
Tom, T., 2000. Monoamine oxidase-B inhibitors in the treatment of Alzheimers disease. Neurobiol. Aging 21, 343–348.
Virginia, M.Y.L., 2002. Amyloid binding ligands as Alzheimer's disease therapies. Neurobiol. Aging 23, 1039–1042.
Wang, Y., Klunk, W., Debnath, M., Huang, G.-F., Holt, D., Shao, L., Mathis, C., 2004. Development of a PET/SPECT agent for amyloid imaging in Alzheimer's disease. J. Mol. Neurosci. 24, 55–62.
Wang, Y., Klunk, W., Huang, G.-F., Debnath, M., Holt, D., Mathis, C., 2002. Synthesis and evaluation of 2-(3′-Iodo-4′-aminophenyl)-6-hydroxybenzothiazole for in vivo quantitation of amyloid deposits in Alzheimer's disease. J. Mol. Neurosci. 19, 11–16.
Wilcock, G.K., Birks, J., Whitehead, A., Evans, S.J.G., 2002. The effect of selegiline in the treatment of people with Alzheimer's disease: a meta-analysis of published trials. Int. J. Geriatr. Psych. 17, 175–183.
Xie, Y., Deng, S., Chen, Z., Yan, S., Landry, D.W., 2006. Identification of small-molecule inhibitors of the Aβ-ABAD interaction. Bioorg. Med. Chem. Lett. 16, 4657–4660.